# Bihormonal Sliding Mode Controller Applied to Blood Glucose Regulation in Patients with Type 1 Diabetes

Manuchi Dansa, Victor Hugo Pereira Rodrigues and Tiago Roux Oliveira
*Dept. of Electronics and Telecommunication Engineering (DETEL)*
*State University of Rio de Janeiro (UERJ)*
Rio de Janeiro, Brazil
manuchid@gmail.com, rodrigues.vhp@gmail.com, tiagoroux@uerj.br

***Abstract*—Control algorithms for a bihormonal artificial pancreas are proposed in such a way that insulin and glucagon actions are incorporated, aiming to avoid hypoglicemic and hiperglicemic episodes. Such control algorithms are utilized in order to ensure the blood glucose regulation in type 1 diabetic patients. The mathematical model utilized has experimental validation and represents the glucose-insulin-glucagon dynamics. First-Order Sliding Mode Controllers with and without Boundary Layer were utilized. One desires to reach, in finite time, an equilibrium condition of the closed-loop control system, even in the presence of disturbances related to feeding. The stability proof is presented assuming that the state is known. In the simulation results, exact differentiators are used in order to recover the information associated with the unmeasured state variables of the system. At last, the performance of two control strategy is evaluated by means of numerical examples.**

***Index Terms*—Uncertain Nonlinear Systems, Biological Mathematics, Bihormonal Control, Diabetes, First-Order Sliding Mode Control.**

## I. Introduction

The pancreas, in addition to its digestive functions, secretes two important hormones, *insulin* and *glucagon*, that are crucial for normal regulation of blood glucose concentration [1]. When the glucose concentration rises above a certain level, insulin is secreted; the insulin in turn causes the blood glucose concentration to drop toward normal. Conversely, a decrease in blood glucose stimulates glucagon secretion; the glucagon then functions in the opposite direction to increase and then steer the glucose back to its normal level.

However, in patients with type 1 diabetes mellitus (T1DM), pancreatic insulin production is impaired, which entails a plenty of risks to these patients health. Tight glucose control reduces the risk of long-term diabetes related complications, such as kidney disease, heart disease, blindness and peripheral vascular and nerve damage. Moreover, conventional methods of self-monitoring of blood glucose and multiple daily injections are challenging for patients and families [2].

Against such a background, an automated closed-loop glucose control system stands out as a target that has been pursued by researchers for the past five decades [3]. Such devices, known as artificial pancreas [4], [5], consist of a glucose sensor, from which data are collected and entered into an algorithm, which in turn compute the amount of insulin to be delivered through a pump.

In modelling drug delivery to human body, certain requirements like finite reaching time and robustness to uncertainties, should be satisfied [6]. In addition, the glucose-insulin dynamics is a complex physiologic system that encompass a number of nonlinear process and therefore cannot be accurately described through linear models [7].

Sliding Mode Control has been proved an efficient technique to provide high-fidelity performance in different control problems for nonlinear systems with uncertainties in system parameters and external disturbances [8].

Concerning the pump actuator for drug delivery, there is a question that has generated much controversy in the artificial pancreas community: to utilize single-hormone systems employing only insulin or to adopt a dual-hormone strategy adding glucagon administration to insulin delivery. Although insulin-only closed-loop systems achieve a much better glycemic control than standard open-loop insulin therapy, it does not completely eliminate the risk of hypoglycaemia [2], [9].

On the other hand, a closed-loop system that employs subcutaneous infusion of both insulin and glucagon has proven its efficacy in preventing and treating hypoglycemia [10], [11]. Moreover, such bihormonal systems would better emulate the function of the endocrine pancreas [12] and, for this sake, will be considered in this paper.

The purpose of this contribution is to introduce closed-loop sliding mode control algorithms capable of regulating the blood glucose concentration in subjects with T1DM through a bihormonal pump. A rigorous stability analysis is carried out by means of Lyapunov's theory taking into account parametric uncertainties in the biological model and unmatched disturbances due to food intake. Numerical simulations illustrate the efficience of the proposed First-order Sliding Mode Control strategy. Implementation aspects concerning chattering alleviation via boundary layers and an output-feedback version of the

This research is financially supported by the following Brazilian development agencies: CAPES, CNPq and FAPERJ.

978-1-5386-4444-7/18/$31.00 ©2018 IEEE

proposed algorithm using higher-order sliding mode (HOSM) differentitators are also discussed and evaluated.

### A. Automatic Control Aspects for Artificial Pancreas

Pumps used for diabetic patients infuse hormone subcutaneously. In this sense, in-silico testing of a dual-hormone control algorithm requires a suitable model that is able to simulate the effects of subcutaneously administered insulin and glucagon [13]. In this essay, we implement the model proposed by [14] extended with glucagon action as proposed by [15].

Although the extended model doesn't specify the type of insulin to be utilized, it suggests the use of a short-acting analog insulin, such as aspart, lispro and glulisine.

Concerning glucagon, the one commercially available nowadays poses risks of occluding the pump catheter due to its instable formulation. Therefore, commercialization of a bihormonal pump will require stable glucagon preparations that can remain in a weareble pump for at least 3-7 days [2].

## II. Mathematical Modeling

Several authors [10], [16], [17] believe a bihormonal closed loop algorithm could provide a safe blood glucose regulation and reduce significantly the risk and time spent in hypoglycemic episodes compared to usual insulin therapy.

The availability of a model that incorporates glucagon as a counterregulatory hormone to insulin would allow more efficient design of bihormonal glucose controllers [10]. In this sense, an extended minimal model was proposed [15] to incorporate the glucagon effect.

For simplicity's sake, we consider in controller design only the reduced model [15]. Such assumption is reasonable since some dynamics among all presented in the extended model are, in general, faster than the dynamics of plasma glucose concentration, insulin action on glucose production and glucagon action on glucose production. Therefore, the dynamics presented in [15] is now represented by:

$$\dot{x}_1(t) = -(S_G + x_2(t) - x_3(t))x_1(t) + S_G G_B + \frac{1}{t_{\max G} V} d(t)\,, \quad (1)$$

$$\dot{x}_2(t) = -p_2(t)x_2(t) + p_2(t)S_I(t)(u^+ - I_B)\,, \quad (2)$$

$$\dot{x}_3(t) = -p_3(t)x_3(t) + p_3(t)S_N(t)(u^- - N_B)\,, \quad (3)$$

$$y(t) = x_1(t)\,, \quad (4)$$

$y(t)$ [mg/dL] is the output variable, $x_1(t)$ [mg/dL] is the plasma glucose concentration, $x_2(t)$ [min$^{-1}$] is the insulin action on glucose production, and $x_3(t)$ [min$^{-1}$] is the glucagon action on glucose production. $V = 1.7$ [dL/kg] is the glucose distribution volume. $u^+ \in \mathbb{R}^+$ [$\mu$U/dL] is the control action and represents the plasma insulin concentration, $u^- \in \mathbb{R}^+$ [pg/dL] is the plasma glucagon concentration, $d(t)$ [mg/kg] is the glucose concentration resulting from ingested meals and $S_G = 0,014$ [min$^{-1}$] is the glucose effectiveness per unit distribution volume. For simplicity's sake, the parameter $t_{maxG} = 69,6$ [min] was assumed constant, since its fluctuations are too slow, in general [15]. All other variables and parameters are described in Table I, followed by its respective units and descriptions. Finally, we remark that if $u^+ \in \mathbb{R}^+$ and $u^- \in \mathbb{R}^+$, it means that the control signals are positive.

The mathematical description of the time-varying parameters is given below:

$$p_2(t) = 0,012\mathbb{1}(t) - 0,0081\mathbb{1}(t-300) + 0,0171\mathbb{1}(t-720) - 0,0091\mathbb{1}(t-1080)\,, \quad (5)$$

$$p_3(t) = 0,017\mathbb{1}(t) - 0,001\mathbb{1}(t-300) + 0,123\mathbb{1}(t-720) - 0,122\mathbb{1}(t-1080)\,, \quad (6)$$

$$S_I(t) = [7,73\mathbb{1}(t) + 0,82\mathbb{1}(t-300) - 1,73\mathbb{1}(t-720) + 0,91\mathbb{1}(t-1080)] \times 10^{-4}\,, \quad (7)$$

$$S_N(t) = [1,38\mathbb{1}(t) + 0,58\mathbb{1}(t-300) - 1,15\mathbb{1}(t-720) + 0,57\mathbb{1}(t-1080)] \times 10^{-4}\,, \quad (8)$$

$$I_B(t) = 11,01\mathbb{1}(t) + 8,75\mathbb{1}(t-300) - 9,73\mathbb{1}(t-720) + 0,98\mathbb{1}(t-1080)\,, \quad (9)$$

$$N_B(t) = 46,30\mathbb{1}(t) + 1,83\mathbb{1}(t-300) + 11,10\mathbb{1}(t-720) - 12,93\mathbb{1}(t-1080)\,, \quad (10)$$

where $\mathbb{1}(t)$ represents the unit step function. The delay in the unit step function is measured in minutes. Therefore, the functions $\mathbb{1}(t-300)$, $\mathbb{1}(t-720)$ and $\mathbb{1}(t-1080)$ denote changes in parameters (5)–(10) at 5:00, 12:00 and 18:00, respectively. The maximum and minimum parameters values (5)–(10) are given by:

$$0,0039 \leq p_2(t) \leq 0,021\,, \quad (11)$$

$$0,016 \leq p_3(t) \leq 0,139\,, \quad (12)$$

$$6,82 \times 10^{-4} \leq S_I(t) \leq 8,55 \times 10^{-4}\,, \quad (13)$$

$$0,81 \times 10^{-4} \leq S_N(t) \leq 1,96 \times 10^{-4}\,, \quad (14)$$

$$10,03 \leq I_B(t) \leq 19,76\,, \quad (15)$$

$$46,30 \leq N_B(t) \leq 59,23\,. \quad (16)$$

During the development of the stability analysis, the system parameters will be considered uncertain in such a way that its bounds are known and described by

$$\underline{p_2} < p_2(t) < \overline{p}_2\,, \quad \underline{p_3} < p_3(t) < \overline{p}_3\,, \quad (17)$$

$$\underline{S_I} < S_I(t) < \overline{S}_I\,, \quad \underline{S_N} < S_N(t) < \overline{S}_N\,, \quad (18)$$

$$\underline{I_B} < I_B(t) < \overline{I}_B\,, \quad \underline{N_B} < N_B(t) < \overline{N}_B\,, \quad (19)$$

$$\underline{t_{\max G}} < t_{\max G}\,, \quad G_B < \overline{G_B}\,, \quad \underline{V} < V\,, \quad (20)$$

$$\underline{S_G} < S_G < \overline{S_G}\,. \quad (21)$$

Furthermore, we assume that

$$|d(t)| < \overline{d}\,, \quad |\dot{d}(t)| < \dot{\overline{d}}\,, \quad (22)$$

where $\overline{d}$ and $\dot{\overline{d}}$ are positive known constants for which (22) is satisfied, except for a zero measure set in the sense of Lebesgue

At last, a couple of remarks concerning the hormones units are presented. Glucagon levels are reported as picogram per milliliter (pg/mL). Insulin is administrated in units, abbreviated U (international units). One unit of insulin is defined as the amount of insulin that will lower the blood glucose of a healthy 2 kg rabbit that has fasted for 24 hours to 45 mg/dL within 5 hours [18].

Proceeding forward, we present the control objective and the methodology utilized in order to reach it. The tools explored for this purpose will be duly discussed.

TABLE I
DESCRIPTION OF EXTENDED MINIMAL MODEL PARAMETERS.

| Parameters | Description |
|---|---|
| $S_G$ [min$^{-1}$] | glucose effectiveness per unit distribution volume |
| $G_B$ [mg/dL] | basal plasma glucose concentration |
| $t_{\max G}(t)$ [min] | time-to-maximum glucose absorption |
| $V$ [dL/kg] | glucose distribution volume |
| $p_2(t)$ [min$^{-1}$] | rate of disappearance of the interstitial insulin effect |
| $S_I(t)$ [min$^{-1}$ per $\mu$ U/mL] | insulin sensitivity |
| $I_B(t)$ [mU/dL] | basal plasma insulin concentration |
| $p_3(t)$ [min$-1$] | rate constant describing the dynamics of glucagon action |
| $S_N(t)$ [min$^{-1}$ por pg/mL] | glucagon sensitivity |
| $N_B(t)$ [pg/mL] | basal plasma glucagon concentration |

## III. CONTROL OBJECTIVE AND METHODOLOGY

The goal of this project is to ensure the regulation of glycemia in a patient with T1DM. Mathematically, it can be represented through output error stabilization:

$$e(t) = G_B - x_1(t)\,, \tag{23}$$

where $G_B = 90$ mg/dL represents the desired setpoint. This value was chosen so that the glycemia of the patient with T1DM remained within the limits considered safe by the medical community: $80$ and $100$ mg/dL [1].

Among all the nonlinear control strategies available, we decided to work with Sliding Modes Controllers (SMC). The main advantage of a SMC relies on the fact that its design does not demand the precise knowledge of the model to be controlled. For controller design, it is sufficient that the upper and lower bounds of the plant parameters are known. Knowledge of upper bounds for disturbances is also required. In this sense, the proposed algorithm is said to be robust with respect to parametric uncertainties and exogenous disturbances like food intake.

## IV. BIHORMONAL ACTUADOR AND FOOD INTAKE

### A. Bihormonal Actuador

Sliding mode controllers have two control actions: a positive control action, $u^+$, and a negative control action, $u^-$. In this essay, the positive control action is represented by the amount of insulin administered in the bloodstream, whilst the negative control action is represented by the amount of glucagon administered in the bloodstream. The algorithm decides which hormone should be injected into the patient at each moment, and this decision satisfies the following rule:

$$u^+ = \begin{cases} \varrho\,, & if \quad u > 0 \quad (\text{sgn}(\sigma) < 0) \\ 0\,, & \text{otherwise} \end{cases}\,, \tag{24}$$

$$u^- = \begin{cases} \varrho\,, & if \quad u < 0 \quad (\text{sgn}(\sigma) > 0) \\ 0\,, & \text{otherwise} \end{cases}\,, \tag{25}$$

where $\varrho$ represents the controller modulation function, and $\sigma$ represents the sliding variable. With rules (24)–(25) in mind, one can conclude that insulin and glucagon are never simultaneously administered.

### B. Disturbance - Food Intake

In this research, it is desired that the patient's blood glucose be regulated over a period of $24$ hours, which is equivalent to $1,440$ minutes. In this context, it is required for the patient to maintain a regular diet consisting of three meals a day, scheduled for the following times: 5:00, 12:00 and 18:00. The food intake modeling was proposed in [6], [20] as:

$$\begin{aligned} d(t) =& 80e^{-0,5(t-300)}\mathbb{1}(t-300) + 100e^{-0,5(t-720)}\mathbb{1}(t-720) \\ &+ 70e^{-0,5(t-1080)}\mathbb{1}(t-1080)\,, \end{aligned} \tag{26}$$

where $d(t)$ can be understood as an exogenous disturbance of the system. Therefore, it is assumed that each meal may represent a different rate of appearance of blood glucose. Figure 1 depicts the effect of meal intake over the patient glycemia.

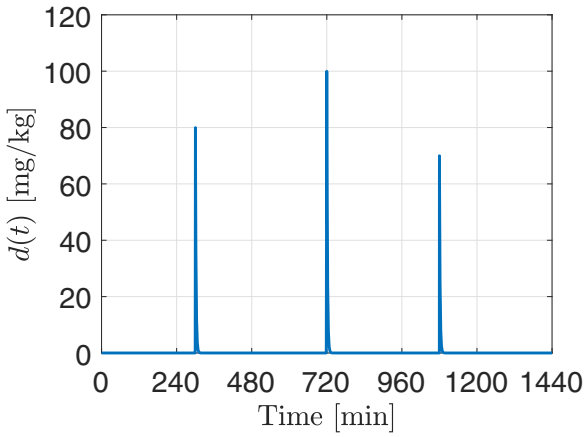


Fig. 1. Glucose concentration resulting from ingested meals along the day.

Hereupon, observe the system (1)–(3). Note the disturbance appears in equation (1), whilst the positive and negative control actions, $u^+$ and $u^-$, respectively, appear in equations (2) and (3).

Thus, the disturbances are said to be *unmatched* [19]. It generates an additional challenge in the controller design, since the control gain will have to upper bound the perturbation and its derivatives in amplitude.

## V. HOSM EXACT DIFFERENTIATOR

Exact differentiators are based on higher order sliding modes (HOSM). This type of tool is able to provide the exact

derivative of the output error $e \in \mathbb{R}$ and ensure the attenuation of small high frequency noises [21]. Its structure is given by:

$$\begin{aligned}
\dot{\zeta}_0 &= v_0 = -\lambda_0 C^{\frac{1}{p+1}} |\zeta_0 - e(t)|^{\frac{p}{p+1}} \operatorname{sgn}(\zeta_0 - e(t)) + \zeta_1, \\
&\vdots \\
\dot{\zeta}_i &= v_i = -\lambda_i C^{\frac{1}{p-i+1}} |\zeta_i - v_{i-1}|^{\frac{p-i}{p-i+1}} \operatorname{sgn}(\zeta_i - v_{i-1}) + \zeta_{i+1}, \\
&\vdots \\
\dot{\zeta}_p &= -\lambda_p C \operatorname{sgn}(\zeta_p - v_{p-1}),
\end{aligned} \tag{27}$$

where $\lambda_i$ are appropriate constants, chosen recursively; $C$ is an appropriate constant, such that $C \geq |e^{(\rho)}(t)|$; the state is described by $\zeta = [\zeta_0, \ \ldots, \ \zeta_{\rho-1}]^T$; and $p = \rho - 1$ represents the order of the differentiator. Therefore, the following equalities

$$\zeta_0 = e(t), \quad \zeta_i = e^{(i)}(t), \quad i = 1, \ldots, p, \tag{28}$$

are established in finite time [21], provided that the signal, $e^{(\rho)}(t)$, be uniformly bounded, as assumed in the HOSM differentiator.

As $\rho = 2$, knowing that the plant has dynamics given by (1)–(4), from the regulation error (23), it is possible to show that the following inequality is satisfied:

$$\begin{aligned}
|\ddot{e}(t)| &= |(-S_G^2 - p_2 S_I I_B + p_3 S_N N_B) x_1(t) \\
&+ S_G G_B (x_2(t) - x_3(t)) - (2S_G + p_2) x_1(t) x_2(t) \\
&+ (2S_G + p_3) x_1(t) x_3(t) - x_1(t) x_2^2(t) - x_1(t) x_3^2(t) \\
&+ 2 x_1(t) x_2(t) x_3(t) + \frac{d(t)}{t_{\max G} V} (S_G + x_2(t) - x_3(t)) \\
&- \frac{\dot{d}(t)}{t_{\max G} V} + S_G^2 G_B + p_2 S_I x_1(t) u^+ - p_3 S_N x_1(t) u^- | \\
&\leq (\bar{S}_G^2 + \bar{p}_2 \bar{S}_I \bar{I}_B + \bar{p}_3 \bar{S}_N \bar{N}_B + 2 \bar{S}_G \bar{G}_B + \frac{2\bar{d}}{\underline{t}_{\max G} \, \underline{\mathrm{V}}} \\
&+ \max\{\bar{p}_2, \bar{p}_3\} + \max\{\bar{S}_I, \bar{S}_N\} \varrho) \chi \\
&+ (4\bar{S}_G + \bar{p}_2 + \bar{p}_3) \chi^2 + 4\chi^3 + \frac{\bar{S}_G \bar{d} + \bar{\dot{d}}}{\underline{t}_{\max G} \, \underline{\mathrm{V}}} + \bar{S}_G^2 \bar{G}_B,
\end{aligned} \tag{29}$$

where the parameters are upper bounded by (17)–(20), the disturbance, $d(t)$, and its derivative, $\dot{e}(t)$, satisfy (22) and the state norm is upper bounded at least locally, by $|x(t)| < \chi$. Assuming that these upper bounds are constant, and are available for designing the controller, an upper bound for the absolute value of the second time-derivative of $e(t)$ can be obtained through

$$\begin{aligned}
C = \Big( & \bar{S}_G^2 + \bar{p}_2 \bar{S}_I \bar{I}_B + \bar{p}_3 \bar{S}_N \bar{N}_B + 2 \bar{S}_G \bar{G}_B + \frac{2\bar{d}}{\underline{t}_{\max G} \, \underline{\mathrm{V}}} \\
& + \max\{\bar{p}_2, \bar{p}_3\} \max\{\bar{S}_I, \bar{S}_N\} \varrho) \chi + (4\bar{S}_G + \bar{p}_2 + \bar{p}_3) \chi^2 \\
& + 4\chi^3 + \frac{\bar{S}_G \bar{d} + \bar{\dot{d}}}{\underline{t}_{\max G} \, \underline{\mathrm{V}}} + \bar{S}_G^2 \bar{G}_B \, .
\end{aligned} \tag{30}$$

Throughout this work, the following exact differentiator will be used:

$$\dot{\zeta}_0 = v_0 = -\lambda_0 C^{\frac{1}{2}} |\zeta_0 - e(t)|^{\frac{1}{2}} \operatorname{sgn}(\zeta_0 - e(t)) + \zeta_1, \tag{31}$$

$$\dot{\zeta}_1 = -\lambda_1 C \operatorname{sgn}(\zeta_1 - v_0), \tag{32}$$

with $\lambda_0 = 5$ and $\lambda_1 = 3$ and gain $C$ given in (30).

The values that have been used in implementing the control system and its parameters are given by: $\mathrm{p}_2 = 0,003$, $\bar{p}_2 = 0,03$; $\mathrm{p}_3 = 0,01$; $\bar{p}_3 = 0,14$; $\underline{\mathrm{S}}_N = 0,8 \times 10^{-4}$; $\bar{S}_N = 2 \times 10^{-4}$; $\underline{\mathrm{S}}_I = 6,8 \times 10^{-4}$; $\bar{S}_I = 8,6 \times 10^{-4}$; $\bar{S}_G = 0,015$; $\bar{N}_B = 60$; $\bar{I}_B = 20$; $\underline{\mathrm{V}} = 1,5$; $\underline{t}_{\max G} = 65$; $\bar{d} = 110$; $\bar{\dot{d}} = 60$ and $\varrho = 100$. These values were chosen from the numeric values of the parameters (5)–(10) which, in turn, can be consulted in [15].

## VI. First-Order Sliding Mode Controller

The sliding mode control is a well documented control technique, and its fundamentals can be found in [19] and [22].

In what follows, we present the local analysis of the first-order sliding mode controller, by means of the ideal sliding variable. Thus, it is assumed, initially, that the error derivatives are available.

*Theorem 1:* Consider the system described by (1)–(4) and the bounds (17)–(20). Thus, it is possible to find a sliding mode control law, $u$, given by:

$$u = -\varrho \operatorname{sgn}(\sigma(t)), \quad \varrho > 0, \tag{33}$$

$$\sigma(t) = \dot{e}(t) + l_0 e(t), \quad l_0 > 0, \tag{34}$$

with constant and sufficiently large modulation function, $\varrho$, and sliding variable $\sigma(t)$, such as, the ideal sliding mode, $\sigma(t) = 0$, occurs in finite time $t_s > 0$. Besides, under the sliding regime, the error convergence is exponential ($e(t) = \mathrm{e}^{-l_0(t-t_s)} e(0), \quad \forall t \geq t_s$).

*Proof:* Consider the following candidate Lyapunov function

$$V(t) = \sigma^2(t), \tag{35}$$

where the time-derivative of $V$ is $\dot{V}(t) = 2\sigma(t)\dot{\sigma}(t)$. Thus,

$$\dot{V}(t) = 2\sigma(t)(\ddot{e}(t) + l_0 \dot{e}(t)). \tag{36}$$

Differentiating equation (23) yields

$$\begin{aligned}
\dot{e}(t) = & -\dot{y}(t) = S_G x_1(t) + x_1(t) x_2(t) - x_1(t) x_3(t) \\
& - S_G G_B - \frac{1}{t_{\max G} V} d(t), \\
\ddot{e}(t) = & (-S_G^2 - p_2(t) S_I(t) I_B(t) + p_3(t) S_N(t) N_B(t)) x_1(t) \\
& + S_G G_B (x_2(t) - x_3(t)) - (2S_G + p_2(t)) x_1(t) x_2(t) \\
& + (2S_G + p_3(t)) x_1(t) x_3(t) - x_1(t) x_2^2(t) - x_1(t) x_3^2(t) \\
& + 2 x_1(t) x_2(t) x_3(t) + \frac{1}{t_{\max G} V} (S_G + x_2(t) - x_3(t)) d(t) \\
& - \frac{1}{t_{\max G} V} \dot{d}(t) + S_G^2 G_B + p_2(t) S_I(t) x_1(t) u^+ \\
& - p_3(t) S_N(t) x_1(t) u^- .
\end{aligned} \tag{37}$$

The time-derivative of (34) is given by

$$\begin{aligned}
\dot{\sigma}(t) = & \ddot{e}(t) + l_0 \dot{e}(t) \\
= & (-S_G^2 - p_2(t) S_I(t) I_B(t) + p_3(t) S_N(t) N_B(t)) x_1(t) \\
& + S_G G_B (x_2(t) - x_3(t)) - (2S_G + p_2(t)) x_1(t) x_2(t) \\
& + (2S_G + p_3(t)) x_1(t) x_3(t) - x_1(t) x_2^2(t) - x_1(t) x_3^2(t) \\
& + 2 x_1(t) x_2(t) x_3(t) + \frac{1}{t_{\max G} V} (S_G + x_2(t) - x_3(t)) d(t) \\
& - \frac{1}{t_{\max G} V} \dot{d}(t) + S_G^2 G_B + l_0 S_G x_1(t) + l_0 x_1(t) x_2(t) \\
& - l_0 x_1(t) x_3(t) - l_0 S_G G_B - \frac{l_0}{t_{\max G} V} d(t) \\
& + p_2(t) S_I(t) x_1(t) u^+ - p_3(t) S_N(t) x_1(t) u^- ,
\end{aligned} \tag{38}$$

Therefore, the first derivative of the candidate Lyapunov function is given by:

$$\begin{aligned}\dot{V}(t) =&2\Big\{(-S_G^2 - p_2(t)S_I(t)I_B(t)\\ &+ p_3(t)S_N(t)N_B(t))x_1(t)\sigma(t) + S_G G_B(x_2(t)\\ &- x_3(t))\sigma(t) - (2S_G + p_2(t))x_1(t)x_2(t)\sigma(t)\\ &+ (2S_G + p_3(t))x_1(t)x_3(t)\sigma(t) - x_1(t)x_2^2(t)\sigma(t)\\ &- x_1(t)x_3^2(t)\sigma(t) + 2x_1(t)x_2(t)x_3(t)\sigma(t)\\ &+ \frac{1}{t_{\max G}V}(S_G + x_2(t) - x_3(t))d(t)\sigma(t)\\ &- \frac{1}{t_{\max G}V}\dot{d}(t)\sigma(t) + S_G^2 G_B\sigma(t) + l_0 S_G x_1(t)\sigma(t)\\ &+ l_0 x_1(t)x_2(t)\sigma(t) - l_0 x_1(t)x_3(t)\sigma(t) - l_0 S_G G_B\sigma(t)\\ &- \frac{l_0}{t_{\max G}V}d(t)\sigma(t) + p_2(t)S_I(t)x_1(t)u^+\sigma(t)\\ &-p_3(t)S_N(t)x_1(t)u^-\sigma(t)\Big\}\,. \end{aligned} \tag{39}$$

Equation (39) can be upper bounded by:

$$\begin{aligned}\dot{V}(t) \le 2\Big\{&(S_G^2 + p_2(t)S_I(t)I_B(t)\\ &+ p_3(t)S_N(t)N_B(t))|x_1(t)||\sigma(t)|\\ &+ S_G G_B(|x_2(t)| + |x_3(t)|)|\sigma(t)|\\ &+ (2S_G + p_2(t))|x_1(t)||x_2(t)||\sigma(t)|\\ &+ (2S_G + p_3(t))|x_1(t)||x_3(t)||\sigma(t)|\\ &+ |x_1(t)||x_2^2(t)||\sigma(t)| + |x_1(t)||x_3^2(t)||\sigma(t)|\\ &+ 2|x_1(t)||x_2(t)||x_3(t)||\sigma(t)|\\ &+ \frac{1}{t_{\max G}V}(S_G + |x_2(t)| + |x_3(t)|)|d(t)||\sigma(t)|\\ &+ \frac{1}{t_{\max G}V}|\dot{d}(t)||\sigma(t)| + S_G^2 G_B|\sigma(t)|\\ &+ l_0 S_G|x_1(t)||\sigma(t)| + l_0|x_1(t)||x_2(t)||\sigma(t)|\\ &+ l_0|x_1(t)||x_3(t)||\sigma(t)| + l_0 S_G G_B|\sigma(t)|\sigma(t)\\ &+ \frac{l_0}{t_{\max G}V}|d(t)||\sigma(t)| + p_2(t)S_I(t)x_1(t)u^+\sigma(t)\\ &-p_3(t)S_N(t)x_1(t)u^-\Big\}\,. \end{aligned} \tag{40}$$

Since the system parameters are uncertain, by using the bounds (17)–(21), the inequality (40) can be upper bounded by:

$$\begin{aligned}\dot{V}(t) \le&2\Big\{\Big[(\bar{S}_G^2 + \bar{p}_2\bar{S}_I\bar{I}_B + \bar{p}_3\bar{S}_N\bar{N}_B)|x_1(t)|\\ &+ \bar{S}_G\bar{G}_B(|x_2(t)| + |x_3(t)|)\\ &+ (2\bar{S}_G\bar{p}_2)|x_1(t)||x_2(t)|\\ &+ (2\bar{S}_G + \bar{p}_3)|x_1(t)||x_3(t)| + |x_1(t)|x_2^2(t)\\ &+ |x_1(t)|x_3^2(t) + 2|x_1(t)||x_2(t)||x_3(t)|\\ &+ \frac{1}{\underline{t_{\max G}}\,\underline{V}}(\bar{S}_G + |x_2(t)| + |x_3(t)|)|d(t)|\\ &+ \frac{1}{\underline{t_{\max G}}\,\underline{V}}|\dot{d}(t)| + \bar{S}_G^2\bar{G}_B + l_0\bar{S}_G|x_1(t)|\\ &+ l_0|x_1(t)||x_2(t)| + l_0|x_1(t)||x_3(t)| + l_0\bar{S}_G\bar{G}_B\\ &+\frac{l_0}{\underline{t_{\max G}}\,\underline{V}}|d(t)|\Big]|\sigma(t)| + p_2(t)S_I(t)x_1(t)u^+\sigma(t)\\ &-p_3(t)S_N(t)x_1(t)u^-\sigma(t)\Big\}\,. \end{aligned} \tag{41}$$

The patient receives insulin ($u^+ = \varrho$) if $u > 0$. In this case, $\mathrm{sgn}(\sigma) < 0 \to \sigma = -|\sigma|$ and $u^- = 0$. So, the inequality (40) can be rewritten as:

$$\begin{aligned}\dot{V}(t) \le 2\Big\{&(\bar{S}_G^2 + \bar{p}_2\bar{S}_I\bar{I}_B + \bar{p}_3\bar{S}_N\bar{N}_B)|x_1(t)|\\ &+ \bar{S}_G\bar{G}_B(|x_2(t)| + |x_3(t)|)\\ &+ (2\bar{S}_G + \bar{p}_2)|x_1(t)||x_2(t)|\\ &+ (2\bar{S}_G + \bar{p}_3)|x_1(t)||x_3(t)| + |x_1(t)|x_2^2(t)\\ &+ |x_1(t)|x_3^2(t) + 2|x_1(t)||x_2(t)||x_3(t)|\\ &+ \frac{1}{\underline{t_{\max G}}\,\underline{V}}(\bar{S}_G + |x_2(t)| + |x_3(t)|)|d(t)|\\ &+ \frac{1}{\underline{t_{\max G}}\,\underline{V}}|\dot{d}(t)| + \bar{S}_G^2\bar{G}_B + l_0\bar{S}_G|x_1(t)|\\ &+ l_0|x_1(t)||x_2(t)| + l_0|x_1(t)||x_3(t)| + l_0\bar{S}_G\bar{G}_B\\ &+\frac{l_0}{\underline{t_{\max G}}\,\underline{V}}|d(t)| - p_2(t)S_I(t)x_1(t)\varrho\Big\}|\sigma(t)|\,. \end{aligned} \tag{42}$$

The patient receives glucagon ($u^- = \varrho$) if $u < 0$. In this case, $\mathrm{sgn}(\sigma) > 0 \to \sigma = |\sigma|$ and $u^+ = 0$. So, the inequality (40) can be rewritten as:

$$\begin{aligned}\dot{V}(t) \le 2\Big\{&(\bar{S}_G^2 + \bar{p}_2\bar{S}_I\bar{I}_B + \bar{p}_3\bar{S}_N\bar{N}_B)|x_1(t)|\\ &+ \bar{S}_G\bar{G}_B(|x_2(t)| + |x_3(t)|) + (2\bar{S}_G + \bar{p}_2)|x_1(t)||x_2(t)|\\ &+ (2\bar{S}_G + \bar{p}_3)|x_1(t)||x_3(t)| + |x_1(t)|x_2^2(t) + |x_1(t)|x_3^2(t)\\ &+ 2|x_1(t)||x_2(t)||x_3(t)|\\ &+ \frac{1}{\underline{t_{\max G}}\,\underline{V}}(\bar{S}_G + |x_2(t)| + |x_3(t)|)|d(t)|\\ &+ \frac{1}{\underline{t_{\max G}}\,\underline{V}}|\dot{d}(t)| + \bar{S}_G^2\bar{G}_B + l_0\bar{S}_G|x_1(t)|\\ &+ l_0|x_1(t)||x_2(t)| + l_0|x_1(t)||x_3(t)| + l_0\bar{S}_G\bar{G}_B\\ &+\frac{l_0}{\underline{t_{\max G}}\,\underline{V}}|d(t)| - p_3(t)S_N(t)x_1(t)\varrho\Big\}|\sigma(t)|\,. \end{aligned} \tag{43}$$

Since $x_1$ stands for glucose, it is straightforward to conclude that $x_1 > 1 \quad \forall t$. Therefore, the inequalities (42) and (43) can be upper bounded by

$$\begin{aligned}\dot{V}(t) \le 2\Big\{&(\bar{S}_G^2 + \bar{p}_2\bar{S}_I\bar{I}_B + \bar{p}_3\bar{S}_N\bar{N}_B)|x_1(t)|\\ &+ \bar{S}_G\bar{G}_B(|x_2(t)| + |x_3(t)|)\\ &+ (2\bar{S}_G + \bar{p}_2)|x_1(t)||x_2(t)|\\ &+ (2\bar{S}_G + \bar{p}_3)|x_1(t)||x_3(t)| + |x_1(t)|x_2^2(t)\\ &+ |x_1(t)|x_3^2(t) + 2|x_1(t)||x_2(t)||x_3(t)|\\ &+ \frac{1}{\underline{t_{\max G}}\,\underline{V}}(\bar{S}_G + |x_2(t)| + |x_3(t)|)|d(t)||\\ &+ \frac{1}{\underline{t_{\max G}}\,\underline{V}}|\dot{d}(t) + \bar{S}_G^2\bar{G}_B + l_0\bar{S}_G|x_1(t)|\\ &+ l_0|x_1(t)||x_2(t)| + l_0|x_1(t)||x_3(t)| + l_0\bar{S}_G\bar{G}_B\\ &+\frac{l_0}{\underline{t_{\max G}}\,\underline{V}}|d(t)| - \min\{\underline{p}_2, \underline{p}_3\}\min\{\underline{S}_I, \underline{S}_N\}\varrho\Big\}|\sigma(t)|\,. \end{aligned} \tag{44}$$

From (44), an upper bound to time-derivative Lyapunov function can be described by:

$$\begin{aligned}\dot{V}(t) \le 2\Big\{&\Big(\bar{S}_G^2 + \bar{p}_2\bar{S}_I\bar{I}_B + \bar{p}_3\bar{S}_N\bar{N}_B + 2\bar{S}_G\bar{G}_B + l_0\bar{S}_G\\ &+\frac{2}{\underline{t_{\max G}}\,\underline{V}}|d(t)|\Big)|x(t)| + (4\bar{S}_G + \bar{p}_2 + \bar{p}_3 + 2l_0)|x(t)|^2\\ &+ 4|x(t)|^3 + \frac{\bar{S}_G + l_0}{\underline{t_{\max G}}\,\underline{V}}|d(t)| + \frac{1}{\underline{t_{\max G}}\,\underline{V}}|\dot{d}(t)| + \bar{S}_G^2\bar{G}_B\\ &+l_0\bar{S}_G\bar{G}_B - \min\{\underline{p}_2, \underline{p}_3\}\min\{\underline{S}_I, \underline{S}_N\}\varrho\Big\}|\sigma(t)|\,. \end{aligned} \tag{45}$$

The meal disturbance, $d(t)$, and its first time-derivative, $\dot{d}(t)$, are bounded by some real positive number described in (22),

such that,

$$\begin{aligned}\dot{V}(t) \leq 2\Big\{&\Big(\bar{S}_G^2 + \bar{p}_2\bar{S}_I\bar{I}_B + \bar{p}_3\bar{S}_N\bar{N}_B + 2\bar{S}_G\bar{G}_B + l_0\bar{S}_G \\ &+ \frac{2}{\underline{t}_{\text{maxG}}\,\underline{\mathrm{V}}}\bar{d}\Big)|x(t)| + (4\bar{S}_G + \bar{p}_2 + \bar{p}_3 + 2l_0)|x(t)|^2 \\ &+ 4|x(t)|^3 + \frac{\bar{S}_G + l_0}{\underline{t}_{\text{maxG}}\,\underline{\mathrm{V}}}\bar{d} + \frac{1}{\underline{t}_{\text{maxG}}\,\underline{\mathrm{V}}}\bar{\dot{d}} + \bar{S}_G^2\bar{G}_B \\ &+ l_0\bar{S}_G\bar{G}_B - \min\{\underline{p}_2, \underline{p}_3\}\min\{\underline{S}_I, \underline{S}_N\}\varrho\Big\}|\sigma(t)|\,. \end{aligned} \tag{46}$$

Let us define $k_1 = \bar{S}_G^2 + \bar{p}_2\bar{S}_I\bar{I}_B + \bar{p}_3\bar{S}_N\bar{N}_B + 2\bar{S}_G\bar{G}_B + l_0\bar{S}_G + \frac{2}{\underline{t}_{\text{maxG}}\,\underline{\mathrm{V}}}\bar{d}$, $k_2 = 4\bar{S}_G + \bar{p}_2 + \bar{p}_3 + 2l_0$, $k_3 = 4$ and $k_4 = \frac{\bar{S}_G + l_0}{\underline{t}_{\text{maxG}}\,\underline{\mathrm{V}}}\bar{d} + \frac{1}{\underline{t}_{\text{maxG}}\,\underline{\mathrm{V}}}\bar{\dot{d}} + \bar{S}_G^2\bar{G}_B + l_0\bar{S}_G\bar{G}_B$. Thus, equation (46) becomes:

$$\begin{aligned}\dot{V}(t) \leq 2\Big\{&k_1|x(t)| + k_2|x(t)|^2 + k_3|x(t)|^3 + k_4 \\ &- \min\{\underline{p}_2, \underline{p}_3\}\min\{\underline{S}_I, \underline{S}_N\}\varrho\Big\}|\sigma(t)|\,. \end{aligned} \tag{47}$$

It is worth mentioning that the state is bounded, since we are dealing with a biologycal system. Thus, we suppose there exists a known upper bound such that the inequality $|x(t)| < \chi$ is satisfied. Therefore, equation (47) can be rewritten as

$$\begin{aligned}\dot{V}(t) \leq 2\Big\{&k_1\chi + k_2\chi^2 + k_3\chi^3 + k_4 \\ &- \min\{\underline{p}_2, \underline{p}_3\}\min\{\underline{S}_I, \underline{S}_N\}\varrho\Big\}|\sigma(t)|\,. \end{aligned} \tag{48}$$

The modulation function is defined as

$$\varrho = \frac{k_1\chi + k_2\chi^2 + k_3\chi^3 + k_4 + \delta}{\min\{\underline{p}_2, \underline{p}_3\}\min\{\underline{S}_I, \underline{S}_N\}}\,, \quad \delta > 0\,. \tag{49}$$

If (49) is replaced in (48), then we can readily obtain

$$\dot{V}(t) \leq -2\delta|\sigma(t)|\,, \quad t \geq 0\,. \tag{50}$$

Let $\tilde{\sigma}(t) := |\sigma(t)| = \sqrt{V(t)}$ be the auxiliary variable. Thus, we have $\dot{\tilde{\sigma}}(t) = \frac{\dot{V}(t)}{2\sqrt{V(t)}}$. Proceeding forward, we divide both sides of (50) by $2\sqrt{V(t)}$, which implies that

$$\frac{\dot{V}(t)}{2\sqrt{V(t)}} \leq -2\delta\frac{|\sigma(t)|}{2\sqrt{V(t)}}\,, \tag{51}$$

which is identical to

$$\dot{\tilde{\sigma}}(t) \leq -\delta\,, \quad t \geq 0\,. \tag{52}$$

By using the comparison lemma, there exists an upper bound $\bar{\sigma}(t)$ of $\tilde{\sigma}(t)$ that satisfies the differential equation

$$\dot{\bar{\sigma}}(t) = -\delta\,, \quad \bar{\sigma}(0) = \tilde{\sigma}(0) \geq 0\,, \quad t \geq 0\,. \tag{53}$$

Integrating both sides of equation (53) yields

$$\bar{\sigma}(t) - \bar{\sigma}(0) = -\delta t \quad t \geq 0\,. \tag{54}$$

Therefore, the following inequality is valid:

$$\bar{\sigma}(t) = -\delta t + \bar{\sigma}(0)\,, \quad t \geq 0\,. \tag{55}$$

Since $\bar{\sigma} \geq 0$ is continuous, $\sigma(t)$ becomes identically null $\forall t \geq t_1 = \delta^{-1}\bar{\sigma}(0)$. Proceeding forward, we conclude that there exists a finite time $0 < t_s \leq t_1$, where the sliding mode starts such that $\sigma(t) = 0, \forall t \geq t_s$. From (34), one can conclude that $\dot{e} = -l_0 e$ and then the error $e(t)$ converges exponentially to zero. ■

## VII. Simulation Results

In this section, we present the stability analysis of a first-order sliding mode controller in cases where the exact differentiators are used for computing the error derivatives. Two strategies have its performances evaluated: the traditional sliding mode controller, which has a discontinuous control action, and the sliding mode controller with *boundary layer*, whose control action is smooth.

### A. Discontinuous Sliding Mode Controller with Estimate of Sliding Variable Using Exact Differentiator

Although Theorem 1 shows that it is possible to find a constant $\varrho$ that locally guarantees the sliding mode, the control law (33)–(34) cannot be implemented, since signal $\dot{e}$ is not available. Thus, remembering equation (28), the control law is adapted and becomes:

$$u = -\varrho\,\mathrm{sgn}(\hat{\sigma}(t))\,, \quad \varrho > 0\,, \tag{56}$$

$$\hat{\sigma}(t) = \zeta_1(t) + l_0\zeta_0(t)\,, \tag{57}$$

where $\hat{\sigma}(t)$ is an estimate for $\sigma(t)$, using (31) and (32).

In the presented simulations, the controller (56)–(57) was implemented with $\varrho = 100$, $l_0 = 1$ [$\text{min}^{-1}$] and with estimated variables $\zeta_0$ and $\zeta_1$ given by (31)–(32). As for the unit of $\varrho$, it should be mentioned that this constant is measured in [$\mu$Umin /mg] during the positive control action; and it is measured in [$pg/dl$] during the negative control action.

Next, the simulation results are presented for the first-order sliding mode controller.

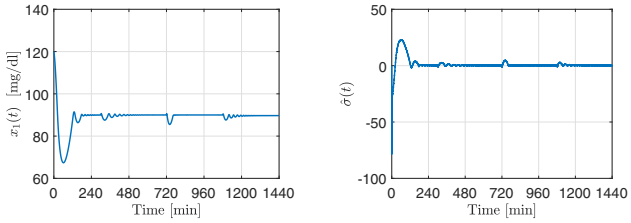


(a) Blood glucose concentration. (b) Sliding variable estimate $\hat{\sigma}$.

Fig. 2. Sliding surface and glycaemia.

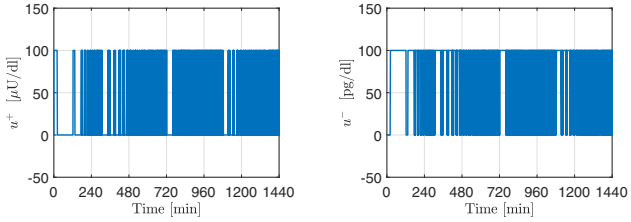


(a) Plasma insulin concentration. (b) Plasma glucagon concentration.

Fig. 3. Insulin and Glucagon.

Figure 2(a) illustrates the ability of the controller to safely regulate the blood glucose and avoid hypoglycemic and hyperglycemic episodes over the period assessed.

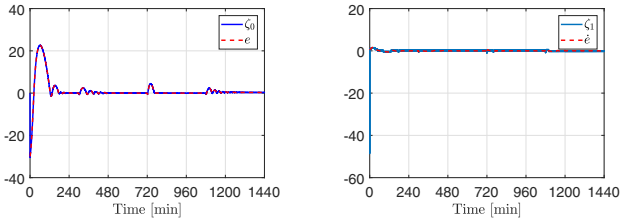


(a) Comparison between $\zeta_0$ and $e$. (b) Comparison between $\zeta_1$ and $\dot{e}$.

Fig. 4. Exact differentiator.

Figures 3(a) and 3(b) demonstrate the role of bi-hormonal actuator, in which $u^+$ stands for insulin and $u^-$ represents the glucagon.

Figures 4(a) and 4(b) attest in favour of the transient briefness of variables $\zeta_0$ and $\zeta_1$. Therefore, the ideal sliding variable $\sigma$ can be constructed from $\hat{\sigma}$, which in turn guarantees that the ideal sliding mode $\sigma = 0$ is reached. It is noteworthy that the signals illustrated in Figure 4(a) are measured in [mg/dL], whilst the signals represented in Figure 4(b) are measured in [mg/dL$^{-1}$ min$^{-1}$].

### *B. Sliding Mode Controller with Estimate of Sliding Variable Using Exact Differentiator and Boundary Layer*

There are some problems that are intrinsic to the traditional sliding mode controller, such as: discontinuous control action and the so-called *chattering* effect. In order to mitigate these effects, we utilize the boundary layer technique [23].

The boundary layer implementation occurs through the the control law design. In this sense, instead of using the relay, we use a control action given by the following law:

$$u = -\varrho \frac{\hat{\sigma}}{|\hat{\sigma}| + \delta}, \tag{58}$$

where $0 < \delta < 1$. Proceeding this way, attenuation of chattering effect is expected to be achieved.

As is evident from Figures 5(a) and 5(b), the controller performance is acceptable and the chattering effect was vanished from control action.

In the remaining aspects, the issues that are to be underscored in Figures 6 and 7 are not different from those referred to Figures 3 and 4, respectively.

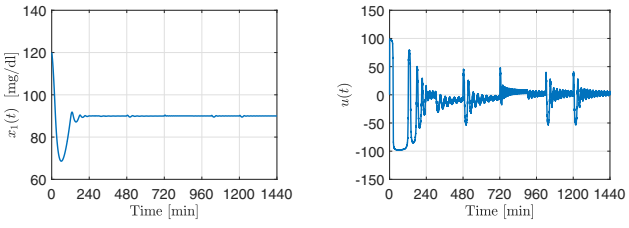


(a) Blood glucose concentration. (b) Controller action.

Fig. 5. Glycaemia and Control Action.

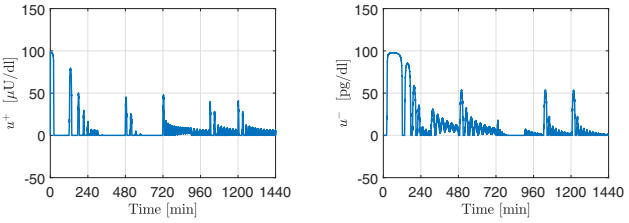


(a) Plasma insulin concentration. (b) Plasma glucagon concentration.

Fig. 6. Insulin and Glucagon.

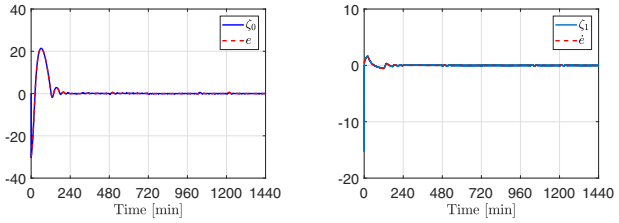


(a) Comparison between $\zeta_0$ and $e$. (b) Comparison between $\zeta_1$ and $\dot{e}$.

Fig. 7. Exact Differentiator.

## VIII. Conclusion

In this work, a first-order sliding mode control strategy was used in order to safely regulate the blood glucose concentration of a T1DM patient. From a control point of view, this is a challenging problem, since the process is represented by a nonlinear, time-varying plant where the parameters where considered uncertain. Meals of varying carbohydrate content are understood as unmatched disturbances, represented by $d(t)$. Moreover, system output has relative degree $\rho = 2$ with regard to control action, and since the model adopted describes a biological system, the control problem must be treated as a strictly positive strategy.

Such challenges were overcome by means of parametric upper bounds, disturbances upper bounds, an bihormonal actuator and the sliding mode control theory. A rigorous analysis through Lyapunov functions and numerical simulations show that the proposed control strategy was efficient in the glycemic regulation process.

## References

[1] A. Guyton and J. Hall, "Textbook of Medical Physiology," Elsevier, 2016.

[2] P. Bakhtiani, L. Zhao, J. El Youssef, J. Castle and W. Ward, "A review of artificial pancreas technologies with an emphasis on bi-hormonal therapy," John Wiley and Sons: Diabetes, Obesity and Metabolism, vol. 15, pp. 1065–1070, December, 2013.

[3] A. Kadish, "Automation Control of Blood Sugar. Servomechanism for Glucose Monitoring and Control," Am. J. Med Electron, pp. 82–86, 1964.

[4] C. Cobelli, E. Renard and B. Kovatchev, "Artificial Pancreas: Past, Present, Future," American Diabetes Association: Diabetes, vol. 60, pp. 2672–2682, 2011.

[5] B. Bequette, "Challenges and Recent Progress in the Development of a Closed-loop Artificial Pancreas," Elsevier Science: Annual Reviews in Control, vol. 36, 2012.

[6] P. Kaveh and Y. Shtessel, “Blood glucose regulation using higher-order sliding mode control,” Wiley Online Library: International Journal of Robust and Nonlinear Control, vol. 18, pp. 557–569, 2008.
[7] S. Audoly, G. Bellu, L. D’Angio, M. Saccomani and C. Cobelli, “Global identifiability of nonlinear models of biological systems,” IEEE Transactions on Biomedical Engineering, vol. 48, pp. 55–65, 2001.
[8] Y. Shtessel, I. Shkolnikov and M. Brown, “An Asymptotic Second-Order Smooth Sliding Mode Control,”John Wiley and Sons: Asian Journal of Control, vol. 5, pp. 498–504, 2003.
[9] K. Kumareswaran, M. Evans and R. Hovorka, “Artificial pancreas: an emerging approach to treat Type 1 diabetes,” Expert Reviews: Expert Review of Medical Devices, vol. 6, pp. 401–410, July, 2009.
[10] F. El-Khatib, S. Russell, D. Nathan, R. Sutherlin and E. Damiano, “A Bihormonal Closed-Loop Artificial Pancreas for Type 1 Diabetes,” Sci Transl Med, April, 2010.
[11] J. Castle, J. Engle, J. El Youssef, R. Massoud, K. Yuen, R. Kagan and W. Ward, “Novel Use of Glucagon in a Closed-Loop System for Prevention of Hypoglycemia in Type 1 Diabetes,” Diabetes Care, pp. 1282–1287, June, 2010.
[12] F. H. El-Khatib, J. Jiang and E. R. Damiano, “A feasibility study of bihormonal closed-loop blood glucose control using dual subcutaneous infusion of insulin and glucagon in ambulatory diabetic swine,” SAGE Publications: Journal of diabetes science and technology, vol. 3, pp. 789–803, 2009.
[13] V. Bátora, D. Boiroux and M. Hagdrup, “Glucagon Administration Strategies for a Dual-Hormone Artificial Pancreas,” IEEE Transactions on Biomedical Engineering, 2015.
[14] R. Bergman, L. Phillips and C. Cobelli, “Physiologic Evaluation of Factors Controlling Glucose Tolerance in Man – Measurement of Insulin Sensitivity and $\beta$–Cell Glucose Sensitivity from the Response to Intravenous Glucose,” Journal of Clinical Investigation, pp. 1456–1467, December, 2012.
[15] P. Herrero, P. Georgiou and N. Oliver, “A Composite Model of Glucagon-Glucose Dynamics for In Silico Testing of Bihormonal Glucose Controllers,” Journal of Diabetes Science and Technology, July, 2013.
[16] V. Batora, M. Tarnik, J. Murgas, S. Schmidt, K. Norgaard, N. Poulsen, H. Madsen, D. Boiroux and J. Jorgensen, “The contribution of glucagon in an Artificial Pancreas for people with type 1 diabetes,” IEEE: American Control Conference (ACC), pp. 5097–5102, 2015.
[17] S. Russell, F. El-Khatib, D. Nathan, K. Magyar, J. Jiang and E. Damiano, “Blood Glucose Control in Type 1 Diabetes With a Bihormonal Bionic Endocrine Pancreas,” Diabetes Care, pp. 2148–2155, 2012.
[18] R. Hanas, “Insulin-dependent Diabetes in Children, Adolescents and Adults,” Department of Pedriatrics, Uddevalla, Sweden, 1998.
[19] C. Edwards and S. Spurgeon, “Sliding Mode Control: Theory and Applications,” CRC Press, 1998.
[20] A. Hernandez, L. Fridman and A. Levant, “High-order sliding-mode control for blood glucose: Practical relative degree approach,” Elsevier: Control Engineering Practice, vol. 21, pp. 747–758, 2013.
[21] A. Levant, “Higher order sliding modes, differentiation and output-feedback control,” International Journal of Control, vol. 76, pp. 924–941, 2003.
[22] V. I. Utkin, “Sliding mode control design principles and applications to electric drives,” IEEE Trans. Ind. Electron., pp. 23–36, January, 1993.
[23] J. J. E. Slotine and W. Li, “Applied nonlinear control,” Prentice-Hall Englewood Cliffs, NJ, vol. 199, 1991.